АСТРОФИЗИКА

ТОМ 63 МАЙ, 2020 ВЫПУСК 2

NEW OPTICAL AND INFRARED PHOTOMETRIC STUDY OF YOUNG OPEN STAR CLUSTER NGC 7790

A.A.HAROON[1,2], R.M.ALREHAILI[1], H.A.ISMAIL[1,2]

Received 28 August 2019
Accepted 11 March 2020

We present deep CCD photometry ($V \sim 21$ mag) in *BVR* Johnson-Cousin filters supported with 2MASS *JHKs* data set for the open star cluster NGC 7790. The cluster's parameters such as reddening, distance, metallicity and age etc... are derived using two color diagrams in optical and near-infrared bands. These parameters are $E_{B-V} = 0.512 \pm 0.006$, $E_{V-R} = 0.382 \pm 0.005$, $E_{J-H} = 0.337 \pm 0.001$ and $E_{J-Ks} = 0.505 \pm 0.001$ mag, the distance modulus $(m - M)_0 = 12.41 \pm 0.001$ mag, which gives a distance of 3.035 kpc and the metallicity $Z = 0.008$. The age obtained by fitting the observed CMDs with Padova isochrones is 63.95 Myr. From the analysis of 2MASS data, the limiting radius of the cluster is found to be 9.7 ± 0.83 arcmin, it reflects that the cluster is a compact cluster. The dynamical relaxation time of NGC 7790 is also determined and found to be 0.17 of its age, which means that the cluster is dynamically relaxed. Moreover, luminosity and mass functions are also investigated.

Keyword: *NGC 7790: open clusters and associations: cepheids: CEa Cas; CEb Cas; CF Cas*

1. *Introduction*. The open star cluster NGC 7790 is near the Perseus arm at ($\alpha_{2000.0} = 23^h58^m18^s$, $\delta_{2000.0} = 61^o13'05''.4$, $l = 116^o.579$, $b = -0^o.9969$). Mermilliod [1] classified NGC 7790 as an intermediate age star and Lynga [2] classified this cluster as Trumpler Class II2m. NGC 7790 has been the subject of various studies, motivated in large part by the presence of three cepheids CEa Cas, CEb Cas and CF Cas (see [3]), making this cluster an important part in the cosmic distance ladder. Romeo et al. [4] determined the reddening and distance modulus of the cluster which turn out to be $E_{B-V} = 0.54 \pm 0.04$ and $(m - M)_0 = 12.65 \pm 0.15$, respectively. They determined also it's age $(5.0 \pm 1.5) \times 10^7$ yr. Matthews et al. [5] investigated the photometric and radial velocity variations of the cluster cepheid CF Cas, and computed its distance of 3160 ± 160 pc (distance modulus 12.5). Gupta et al. [6] observed the cluster in optical *BVI* photometric passbands and got the $E_{B-V} = 0.51 \pm 0.03$ with distance of 3.3 ± 0.23 kpc. Davidge [7] studied the cluster and determined the color excesses 0.56 ± 0.05, distance modules 12.057 ± 0.01 and an age 60-80 Myr. Almost all the previous studies had got the same results, in addition, they are in the optical passband. So, due to the importance of this cluster

we restudied it both in optical and infrared bands (for the first time) and compared our results with previous studies.

The paper is organized as follows: the CCD optical observations and near infrared data (2MASS) is described in the Section 2. In Section 3 the radial density profile is presented. The field star decontamination algorithm is given in Section 4. The analysis of the color-magnitude diagrams and the derived photometric parameters are given in Section 5. The luminosity function and mass function are described in Section 6, while the mass segregation and dynamical relaxation state of the cluster are described in Section 7. The last section presents summary of our study and conclusion.

2. *The CCD optical observations and near infrared data (2MASS).*

2.1. *The CCD optical observations*. CCD *BVR* observations for the open star cluster NGC 7790 were carried out with the 188 cm reflector telescope at Newtonian focus (f/4.9) during one night on November 30, 2010. The telescope is operated by Kottamia observatory, astronomy department of NRIAG, Egypt. It was equipped with a 2k x 2k EEV 42-40 CCD camera, its pixel size of 13.5 μm. The telescope and this CCD camera give us a square field of view of about 10 x 10 arcmin^2 on the sky with a scale of 0.30 arcsec per pixel, more information about the capabilities of Kottamia telescope are presented in [8]. Table 1 lists the observation log of 36 science exposures. Bias and twilight flat field frames were taken in the three filters. The observations of the standard stars in the selected area SA 107 [9] have been performed to calibrate the target observations.

Table 1

LOG OF OBSERVATIONS

Date	Filter	No. of exp.	Air mass range	Exp. time (sec)
Nov. 30, 2010	*B*	12	1.002 - 1.098	120
Nov. 30, 2010	*V*	12	1.009 - 1.094	120
Nov. 30, 2010	*R*	12	1.010 - 1.091	120

The standard CCD reduction processing was done under IRAF software for the cluster and standard stars CCD frames. These processes include bias subtraction, flat field corrections, removal of cosmic rays, aperture and point spread function photometry and magnitude transformation to the standard system.

We determined the calibration coefficients that transform the instrumental magnitudes to the standard ones using the observation of the standard stars. The transformation equations are in the following form:

$$b = B + z_b + k_b X + a_b (B - V)$$

$$v = V + z_v + k_v X + a_v (B - V)$$

$$r = R + z_r + k_r X + a_r (V - R)$$

Where B, V, R, and b, v, r are the standard and the instrumental magnitudes respectively. X is the airmass, while z_b, z_v, z_r and k_b, k_v, k_r are the photometric zero points and the extinction coefficients in B, V, R filters respectively. The a_b, a_v, a_r, are the color coefficients. The values of extinction coefficients, the color coefficients and the photometric zero points in their corresponding filters are given in Table 2.

Table 2

THE ZERO POINT, COLOR AND EXTINCTION COEFFICIENTS FOR EACH FILTER

Parameter / Filter subscript	k	a	z
b	0.35	0.004	3.02
v	0.17	0.002	2.80
r	0.08	0.001	2.71

2.2. *Near-Infrared Data (2MASS)*. The 2MASS photometric data on near-infrared *JHKs* filters were extracted from Vizier web page[1] for the star cluster NGC 7790. Due to the small area of the optical field of view, we investigate the cluster structure based only on the 2MASS data. Starting with determination of the cluster center by constructing a rectangular strip around the cluster center (visually determined) in α and δ direction with a side of one degree wide, we count the stars in each strip to build the frequency distribution in both directions. These histograms were fitted by a Gaussian function, whereas the location of maximum number of stars (peak) indicates the new cluster center, as illustrated in Fig.1 and listed in Table 3. The 2MASS data are extracted again, for further investigation, centered on the new coordinates with an aperture radius of 20 arcmin. The large

Table 3

THE CENTER COORDINATES COMPARING WITH PREVIOUS WORK

	[10]	[6]	Recent work
RA_{J2000}	$23^h55^m0^s.9$	$23^h54^m12^s$	$23^h58^m18^s.0$
DE_{J2000}	60°56'	+60°57'	61°13'05".4
l	116°	116°.6	116°.579
b	-1°	-1°	-0°.9969

[1] *http://vizier.u.strasbg.fr/viz.bin/VizieR*

extraction area around each cluster enables us to determine statistically the surface density distribution of the field stars in the cluster outskirt.

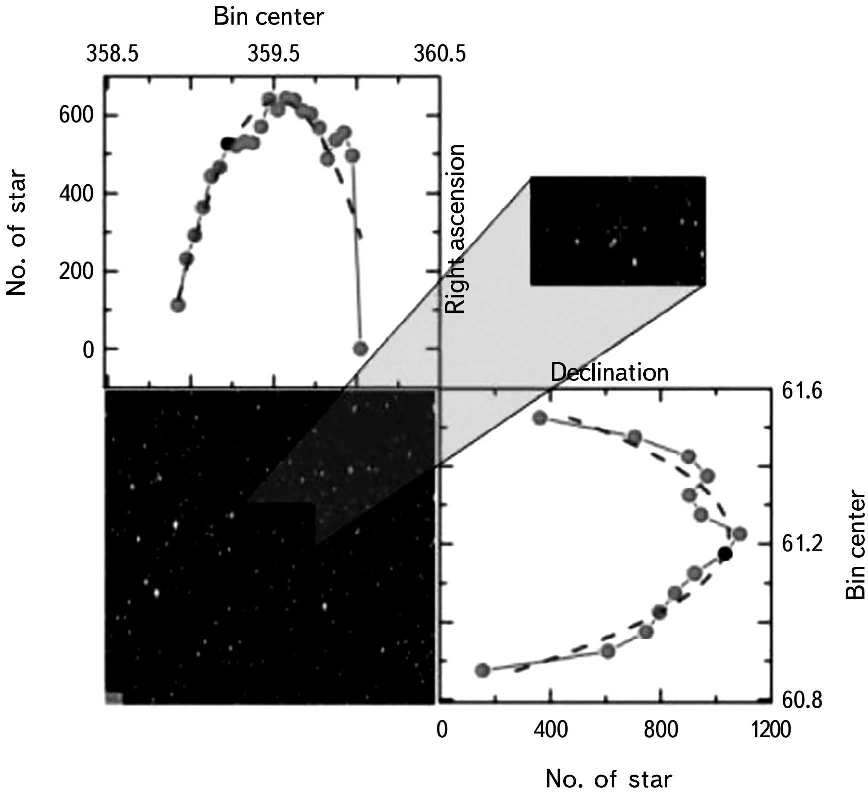

Fig.1. The Gaussian fitting profiles of star counts across right ascension α and declination δ for the cluster. The peak's position of the profile gives the cluster's center.

3. *Radial density profile (RDP)*. The stellar density distribution of a cluster is a result of the internal and external dynamical process. The radial density profile (RDP), the number of stars per unit area at different radius from cluster's center outward, is an observational tool that reflects the dynamical events acting on the cluster and it enables us to determine the angular size of the cluster. The radial density profile is determined through counting the stars in concentric rings around the new cluster's center. We calculated the density of each ring by dividing the number of stars in the ring by its area. The ring radius was chosen to be ranged from 0.25 to 1.5 arcmin; to avoid the smallest number of the stars in the ring and then the density profile was chosen by visual inspection of the data for each ring bin size. The density profile must represent the well exponential decreasing of the cluster surface density outward from its center, as well as the

constancy of the dense background after the cluster limit. We applied the empirical King model [11] to fit the observed RDP. The King model of the density function equation is in the following form:

$$\rho(r) = f_{bg} + \frac{f_0}{1 + \left(\frac{r}{r_{core}}\right)^2},$$

where r_{core}, f_0, and f_{bg} are the core radius, the central surface density and background surface density and their values of $r_{core} = 2.036 \pm 0.167$, $f_0 = 8.606 \pm 0.415$ and $f_{bg} = 9.899 \pm 0.121$ respectively. The core radius is the cluster radius at which the central surface density drops to its half value. We suppose that the background star density lies within the lines representing the standard deviation of the background density level, therefore we define the cluster limits (cluster limited radius; $r_{\lim} = 9.7 \pm 0.83$ arcmin) at the intersection of the King profile with the upper limit of the density standard deviation line (see Fig.2). This value is larger than the value obtained by [6] who had $r_{\lim} = 3.7 \pm 0.2$ arcmin, whereas Lynga [2] determined the RDP = 2.5 arcmin.

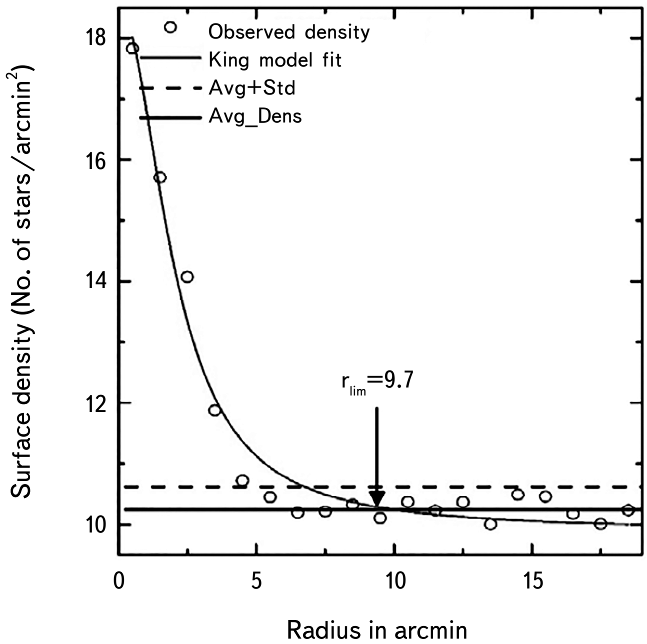

Fig.2. The radial density profile for the cluster. The solid curve denotes the fitting with King model, while the dashed lines mark the level of the background density and its standard deviation.

4. *Membership of star cluster*. The field stars decontamination from a star cluster is an essential task to obtain an accurate photometric study for star

clusters. To decontaminate the field stars, we used the kinematic approaches based on the availability of the kinematic data such as proper motion and radial velocities [12,13]. We used the kinematical method because these kinematic data for the cluster are available to determine the cluster membership and cleaning the clusters from field star contamination. In this technique, we use TOPCAT[2] program (Tool for Operations on Catalogues And Tables). Moreover, it is also interactive graphical viewer and editor for tabular data. To summarize this process, by using the proper motion component in α (pmRA) and δ (pmDE), we build two histograms. In respective histograms, the highest count of stars in both (pmRA) and (pmDE) represents the range of the cluster star members [13]. These stars share almost the same proper motion values. Then by selecting the range for both (pmRA) and (pmDE) around the histogram peak, the star members are examined. To confirm this range, a proper motion vector point diagram (PMVPD) which is a plot of (pmRA) and (pmDE) [14] is employed in color-magnitude diagram Fig.3.

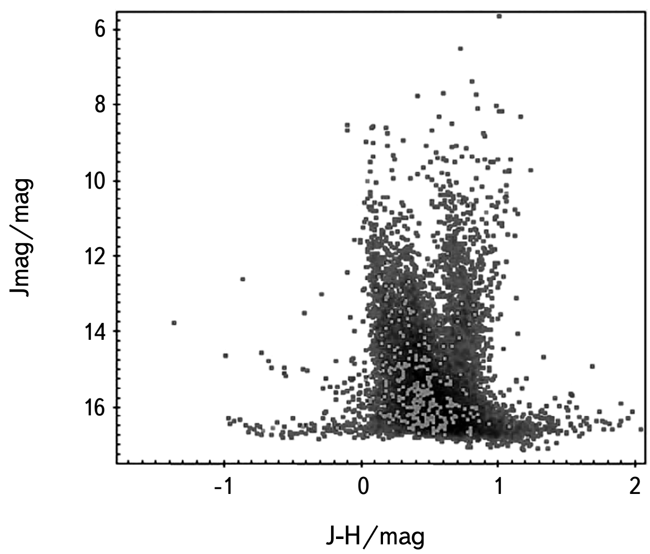

Fig.3. The NGC 7790 star members (light squares), while the field stars (dark squares).

5. *The color-magnitude diagrams.* The Color-Magnitude Diagram (CMD) for a star cluster enables us to determine its age, reddening and distance. So, two optical (V, $B-V$), and (V, $V-R$) and two infrared (J, J-H & Ks, J-Ks) CMDs for the total number of the observed stars in the decontaminated cluster region ($r < r_{\mathrm{lim}}$) are constructed for the cluster NGC 7790 and presented in Fig.4, 5. To derive the fundamental parameters of this cluster, these CMDs were fitted with

[2] *http://www.star.bris.ac.uk/~mbt/topcat/*

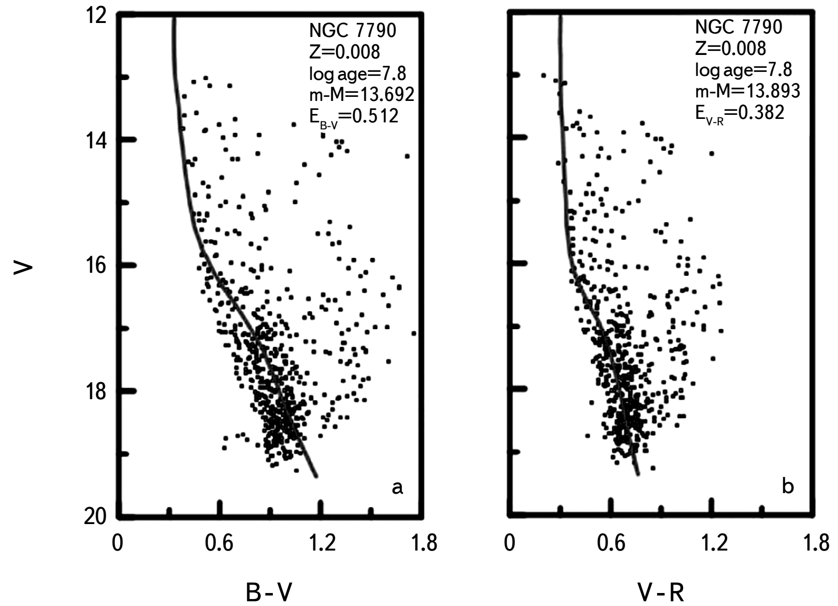

Fig.4. Color magnitude diagrams a) (V, B-V) and b) (V, V-R), the solid curve represents the best fitted Padova isochrones with $Z = 0.008$ and age of 63.95 Myr.

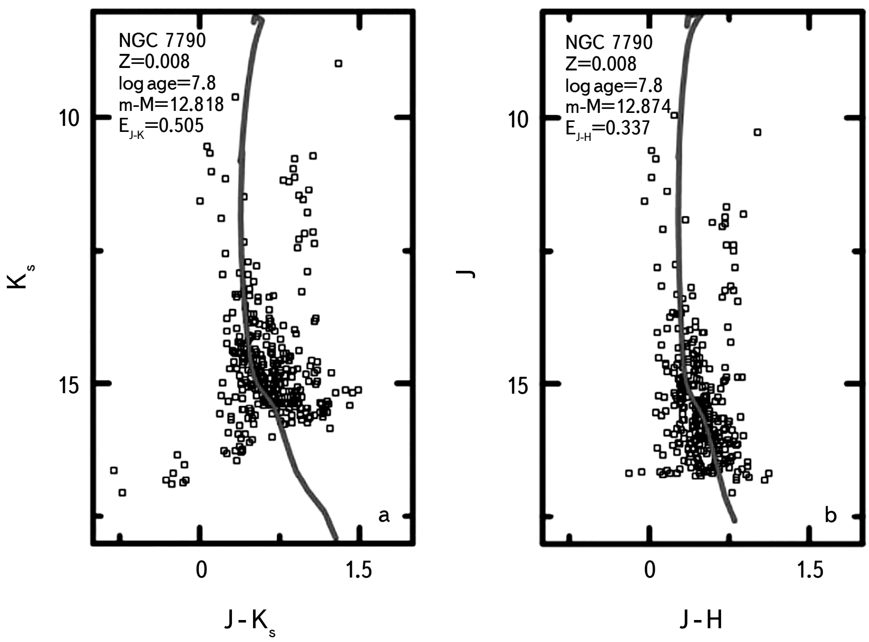

Fig.5. 2MASS CMDs; a) (Ks, J-Ks) and b) (J, J-H), the solid curve represents the best fitted Padova isochrone with $Z = 0.008$ and age of 63.95 Myr.

several theoretical Padova isochrones[3] [15] in different metallicities and ages in steps of 0.05 in the logarithm of age. This step was adopted as a typical uncertainty of the log age. We got a good fit for all CMDs by visual inspection with the isochrone of the metallicity $Z = 0.008$, and the corresponding age of 63.95 Myr. The optical and infrared color excesses are determined from CCDs fitting, and using the relations of [16]. The optical color excess $E_{B-V} = 0.512 \pm 0.006$, $E_{V-R} = 0.382 \pm 0.005$ and the absolute distance modulus $(m - M)_0 = 12.41 \pm 0.001$ mag, gives a distance of 3.035 kpc. These results agree well with that given by [6], $E_{B-V} = 0.51 \pm 0.03$ mag and the distance of 3.3 ± 0.23 kpc. In [16] were presented the color excess values for 2MASS photometric system, which enable us to obtain the following results: $E_{J-H} = 0.337 \pm 0.001$, $E_{J-K} = 0.505 \pm 0.001$ and $A_V = 3.317$ where $R_V = A_V / E_{B-V} = 3.1$ is adopted.

6. *The luminosity and mass function.* The number of stars in a cluster with different absolute luminosities describes the stellar luminosity function (LF)

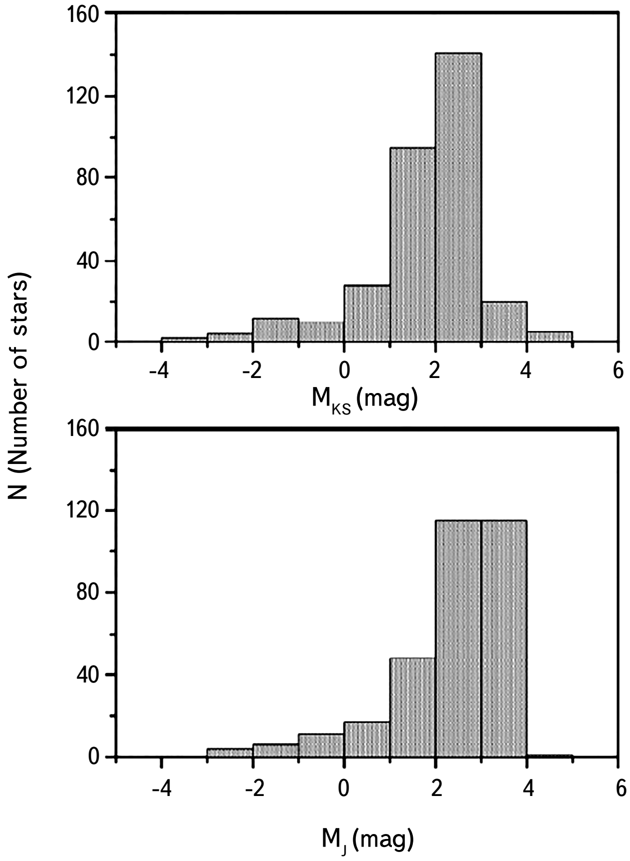

Fig.6. The cluster luminosity function.

---

[3] *http://pleiadi.pd.astro.it/*

of the cluster. So, we transformed the J apparent magnitude to absolute magnitude using the cluster's distance modulus, then the frequency distribution of the J absolute magnitude has been obtained, as shown in Fig.6. This luminosity function is transformed to the mass function based on the dependence of the mass on the luminosity given in the selected theoretical Padova isochrones [15].

In the present work, the absolute magnitude and the masses for the adopted isochrone with metallicity $Z = 0.008$ are used to construct the relation between $M/M_{\odot}$ and absolute magnitude M_J. The relation is a polynomial function of the second degree, used to determine masses of the cluster from the observed absolute magnitude M_J. Then a histogram for the number of stars as a function of mass interval is constructed and presented in Fig.7. The mass frequency distribution is linearly fitted with the slope value of -2.36, this value is closer to that of [17] obtained by study of the IMF for massive stars. Note that, the steep slope of the IMF indicates that the number of low-mass stars is greater than the high-mass ones. The masses are integrated to compute the total mass of the cluster $M \approx 1316 M_{\odot}$.

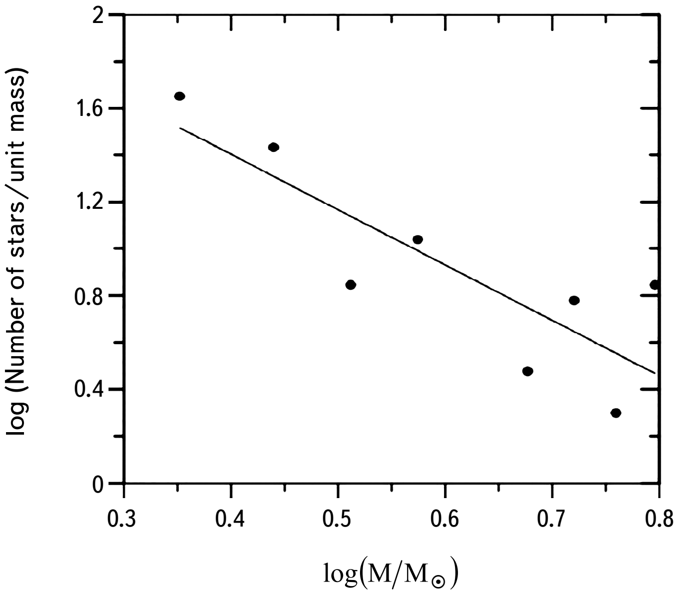

Fig.7. The mass frequency distribution is linearly fitted with the slope value of -2.36.

7. *Mass segregation and dynamical relaxation time*. The dynamical relaxation T_E is the time in which the individual stars exchange energies and their velocity distribution approach a Maxwellian equilibrium. An examination of the distribution of masses of the stars along the radius of the cluster showed a clear segregation of mass in the cluster, with the massive stars located in the central

part of the cluster. To check whether the existing mass segregation is due to dynamical evolution or the imprint of the star formation process, we need to estimate the dynamical relaxation time. Through the dynamical relaxation time, the low mass stars in a cluster may possess the largest random velocities trying to occupy a larger volume than the high mass stars (see [18]). Here, the relation given by [19] is used to compute the dynamical relaxation time for the cluster.

$$T_E = \frac{8.9\times10^5\, N^{1/2} R_h^{3/2}}{\langle m\rangle^{1/2}\log(0.4N)},$$

where R_h is the radius containing half the cluster mass, N is the number of cluster members and $\langle m\rangle = 2.867\pm1.49\,M_\odot$ is the average mass of the cluster stars. Considering the R_h is equal to half of the cluster radius in linear units, we have calculated dynamical relaxation time ($T_E = 10.5\pm2.9$ Myr). Comparing the values of T_E with the cluster ages, we find Age/$T_E = 6.1\pm1.6$. Since the values of the T_E are smaller than the estimated cluster ages, it may be inferred that the cluster is dynamically relaxed and the mass segregation effect due to dynamical evolution must be important. The cluster relaxation time is much shorter than its age (~0.17 of its age), that means the cluster is highly dynamically relaxed.

8. *Conclusions*. New CCD *BVR* observation and *JHKs* 2MASS data for the open star cluster NGC 7790 are used to determine the cluster structure and photometric parameters. The infrared dataset reveals NGC 7790 is a compact open cluster, with the limited size of the cluster; its radius is limited to 9.7 ± 0.83 arcmin which is about 2.6 time more than [6], and its core radius by 2.036 ± 0.167 arcmin. Our estimates of the cluster distance 3.035 kpc, age 63.95 Myr and poor metallicity of $Z=0.008$ are very close to that determined earlier (Table 4). Both age and distance estimates for the cepheid variables are consistent with the present determination. However, the interstellar reddening, $E_{B-V}=0.512\pm0.006$ agrees well with the previous studied. In addition, we also found the infrared color excess $E_{J-K}=0.505\pm0.001$ and $E_{J-H}=0.337\pm0.001$ and the visual absorption

Table 4

DETERMINED PARAMETERS FROM CMD FOR NGC 7790 COMPARING WITH PREVIOUS STUDIES

	[4]	[6]	[7]	Recent work Optical	Recent work 2MASS
Z	0.01	0.008	0.019	0.008	0.008
Age	50 Myr	120 ± 20 Myr	60 - 80 Myr	63.95 Myr	63.95 Myr
$E(B\text{-}V)$	0.54 ± 0.04	0.51 ± 0.03	0.56 ± 0.05	0.512 ± 0.006	1.07 ± 0.27
$(m\text{-}M)_0$	12.65 ± 0.15	12.6 ± 0.15	12.057 ± 0.01	12.41	12.211 ± 0.005
d, kpc	-	3.3 ± 0.23	3.160 ± 1.6	3.035	2.768 ± 0.006

$A_V = 1.671 \pm 0.003$.

From the investigation of the mass function within the cluster, we estimated total mass of the cluster membership of $\approx 1316 M_\odot$. In addition, the cluster dynamical relaxation time ($T_E = 10.5$ Myr) is about 0.17 of its age (63.95 Myr), which means that the cluster is dynamically relaxed.

Acknowledgments. This publication also makes use of data products from the Two Micron All Sky Survey, which is a joint project of the University of Massachusetts and the Infrared Processing and Analysis Center/California Institute of Technology, funded by the National Aeronautics and Space Administration and the National Science Foundation.

[1] Astronomy Department, Faculty of Science, King Abdul Aziz University, Jeddah, KSA, e-mail: aaharoon@kau.edu.sa alrehaili.razan@gmail.com hamedismail6@gmail.com

[2] National Research Institute of Astronomy and Geophysics, Helwan, Cairo, Egypt

НОВОЕ ОПТИЧЕСКОЕ И ИНФРАКРАСНОЕ ФОТОМЕТРИЧЕСКОЕ ИССЛЕДОВАНИЕ МОЛОДОГО ОТКРЫТОГО СКОПЛЕНИЯ ЗВЕЗД NGC 7790

А.А.АРУН[1,2], Р.М.АЛРЕХАЙЛИ[1], Х.А.ИСМАИЛ[1,2]

Представлены глубокая ПЗС-фотометрия ($V \sim 21$ mag) в фильтрах Джонсона-Кузена *BVR,* а также 2MASS *JHK* данные для открытого звездного скопления NGC 7790. Используя двухцветные диаграммы в оптическом и ближнем инфракрасном диапазонах получены такие параметры скопления, как покраснение, расстояние, металличность, возраст и т. д. Этими параметрами являются $E_{B-V} = 0.512 \pm 0.006$, $E_{V-R} = 0.382 \pm 0.005$, $E_{J-H} = 0.337 \pm 0.001$ и $E_{J-Ks} = 0.^m505 \pm 0.^m001$, модуль расстояния $(m-M)_0 = 12.410 \pm 001$, что соответствует расстоянию 3.035 кпк и металличность $Z = 0.008$. Возраст, полученный путем сравнения наблюдаемой диаграммы цвет-величина (CMD) с изохронами Падуи, составляет 63.95 миллиона лет. Анализ данных 2MASS показывает, что предельный радиус скопления составляет 9.7 ± 0.83 угл. мин., что указывает на компактность скопления. Время динамической релаксации NGC 7790 также определено и составляет 0.17 его возраста, что означает, что в скопление произошла динамическая релаксация. Кроме того, были исследованы функции светимости и массы.

Ключевые слова: *NGC 7790: открытые скопления и ассоциации: цефеиды: CEa Cas; CEb Cas; CF Cas*

REFERENCES

1. *J.C.Mermilliod*, Astron. Astrophys. Suppl. Ser., **97**, 235, 1981.
2. *G.Lynga*, Catalogue of open cluster data, 5th edition, 1/1 S7041, Centre de Donnees Stellaires, Strasbourg, 1987.
3. *M.Pedreros*, *B.F.Madore*, *W.L.Freedman*, Astrophys. J., **286**, 563, 1984.
4. *G.Romeo*, *A.Bonifazi*, *F.F.Pecci et al.*, Mon. Not. Roy. Astron. Soc., **240**, 459, 1989.
5. *J.M.Matthews*, *W.P.Gieren*, *J.C.Mermilliod et al.*, Astron. J., **110**, 2280, 1995.
6. *A.C.Gupta*, *A.Subramaniam*, *R.Sagar et al.*, Astron. Astrophys. Suppl. Ser., **145**(3), 365, 2000.
7. *T.J.Davidge*, Astrophys. J., **761**(2), 155, 2012.
8. *Y.A.Azzam*, *G.B.Ali*, *H.A.Ismail et al.*, Third UN/ESA/NASA (Workshop on the International Heliophysical Year 2007 and Basic Space Science), 175A, 2010.
9. *A.U.Landolt*, Astron. J., **104**, 340, 1992.
10. *J.D.Lee*, *S.G.Lee*, J. Korean Astron. Soc., **32**(2), 91, 1999.
11. *I.R.King*, Astron. J., **71**, 64, 1966.
12. *M.H.Slovak*, Astron. J., **82**, 818, 1977.
13. *J.Cabrera-Caño*, *E.J.Alfaro*, Astron. Astrophys., **150**, 298, 1985.
14. *B.F.Jones*, Memorie della Societa Astronomica Italiana, **68**, 833, 1997.
15. *Ch.Bonatto*, *E.Bica*, *L.Girardi*, Astron. Astrophys. **415**, 571, 2004.
16. *M.Fiorucci*, *U.Munari*, Astron. Astrophys., **401**(2), 781, 2003.
17. *E.E.Salpeter*, Astrophys. J., **121**, 161, 1955.
18. *R.D.Mathieu*, *D.W.Latham*, *R.F.Griffin et al.*, Astron. J., 92.1100M, 1986.
19. *J.Spitzer*, *M.Hart*, Astrophys. J., **164**, 399, 1971.